Grenze International Journal of Engineering and Technology, June Issue

Coil Design for a 3.7kW WPT Electric Vehicle Charger

Raja Vidya[1] and B.K. Keshaven[2]
[1]Department of Electrical and Electronics Engineering, RV College of Engineering®, Bangalore, India
Email: rajavidya@rvce.edu.in
[2]Department of Electrical and Electronics Engineering, PES University, Bangalore, India
Email: keshavanbk@pes.edu

***Abstract*—In recent times, one of the most promising research areas in EV technology is Wireless power transfer (WPT). It has the potential to solve few drawbacks of the current EV technology such as conductive charging with awkwardly long orange colored high voltage chords, limited battery endurance, range anxiety and lack of charging infrastructure facilities [1–5]. Various Circuit formulations like inductive or capacitive or magnetic resonance coupling techniques have been proposed for WPT. These various techniques try to transfer power within a couple of centimeters using either basic topologies like Series-Series, Series-Parallel, Parallel-Series and Parallel-Parallel or Hybrid topologies (LCC, LCCL, LLC etc) [6–9]. This paper discusses magnetic Resonance technique based WPT system mainly for Circular, Square and Bipolar Coil Structures (Rectangle in Geometry). This paper gives step by step guidance for coil design for three different coil structures to transfer 3.7 kW of power across 180 mm distance. A novel WPT charger will be proposed by comparing the results obtained from the analysis of three different coil structures. The various coil structures are studied by finite element method (FEM) using Ansys Electromagnetics and circuit analysis are done using Simplorer. This is a comprehensive analysis, where each coil configurations are analyzed as bare coils, with ferrites and with ferrites and shielding techniques. The results are compared, and an optimized design is proposed towards charging Electric Vehicles Wirelessly.**

***Index Terms*— Wireless Power Transfer (WPT), Resonance technique, Ansys, Coil Design, Electric Vehicles (EVs).**

I. INTRODUCTION

Of late, Electric Vehicles (EVs) have become very popular globally as EVs reduce pollution and Carbon Dioxide emissions and achieve higher energy efficiency [10-11]. Additionally, with the rapid advancement in the areas related to batteries and charging infrastructure and electric motors helped EVs to get recognized as one of the sustainable and efficient alternatives to conventional vehicles [12-14]. The study on EV technology and the related development in crucial fields such as battery, charging, electric motor and charging infrastructure, has been discussed in the literature [13]. Basically, WPT system can be sub-divided into static wireless charging and mobile wireless charging [15-16]. In static wireless charging technique, the vehicle is parked over a charging mechanism mounted or built alongside on the platform called as transmitter (Tx) and a corresponding charging pad slung on the underside of the chassis of the vehicle called as a receiver (Rx), detects the signal and the vehicle gets charged as shown in Fig 1.

There are multiple ways of placing Transmitter and Receiver, so that charging is of EVs done wirelessly: One way is to place the receiver coils under the chassis of the EV and transmitter coils buried underground, and by

Grenze ID: 01.GIJET.8.2.301

driving the vehicle over these transmitter coils, the EVs can be charged. Another way is to mount the receiver coils vertically just behind the front bumper/grills (Ex: in place of radiators in ICE vehicles) and the transmitter coils embedded in the walls of the garage/charger infrastructure and when the vehicle is parked facing these embedded transmitter coils, the vehicle gets charged.

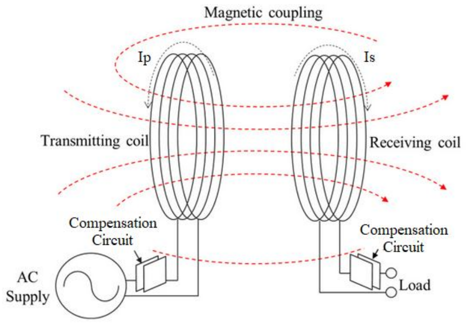

Figure 1. Magnetic Coupling between Transmitter and Receiver Coils

The main downsize of WPT technique is that the technology has lesser power transfer efficiency over a distance compared with conductive charging systems. It has been discussed in literatures that the coupling coefficient (CC) is a key topic of interest in WPT systems, as it determines the maximum output power and has a huge impact on the overall system efficiency [17]. Since CC is proportional to the size of the loosely coupled (LC) transformer at a certain air gap - coil geometry, coil shape, number of turns, width and distance between the turns decides the overall efficiency of the WPT system. To aid in the development of WPT systems, many compensation topologies of resonant circuits and the control methods for the inverters/converters on both side of the charger have been investigated in many literatures. There are two popular topologies for the transmitter and receiver side resonant circuits - series, and parallel connected circuits [18-19]. Each compensation topology has its own positives and negatives. According to the specifications of the application [20–22] – the choice has to be made. The authors [23-24] have discussed magnetic coupling effect as a general design method for the popularly used resonant topologies.

The coupling coils or magnetic pads, which forms the inductive link for transferring power through the air gap [25] makes up a critical part of the WPT system. In the literature [26-27], different types of magnetic pads are available - that can transfer power over large air gaps. These magnetic or charging pads are so called due to the structure of the coil or by the profile of the magnetic field linking between transmitter and receiver. Among the available coil structures, the prominent geometries are the circular, double D and DDQ, where latter is derived by adding quadrature coil to double D, solenoid, bipolar and tripolar pads [28]. The other classification based on the profile of the magnetic field linking with transmitter and receiver, are non-polarized (circular) or polarized (solenoid, DD). DDQ, bipolar and tripolar coils can develop either nonpolarized or polarized magnetic field based on the excitation given to different coils in the charging pad, The difference between a non-polarized charging pad and a polarized charging pad is that a non-polarized charging pad ideally generates and couples perpendicular component of the magnetic flux, whereas polarized charging pad generates and couples magnetic flux which is parallel to one of the dimensions of the charging pad as discussed by authors in [27].

In this paper a Coil design of a 3.7kW Electric Vehicle Charger using WPT Technique at 180mm distance is proposed where a comparative analysis is done with Circular, Square and Bipolar coil structures with charging pads for effective magnetic flux linking and Aluminium shielding. The analysis is carried out using FEM technique in Ansys Maxwell.

II. A 3.7KW ELECTRIC VEHICLE CHARGER DESIGN STEPS

To arrive at 3.7kw Charger, a step by step design procedure must be followed. Fig 2. Depicts the procedure to arrive at a suitable 3.7 kW charger.

Designing a Wireless Transfer System is not frivolous as it must comply complex requirements related to Power transfer limit, efficiency, electromagnetic emissions, dimension of coils, alignment and cost. All these parameters greatly influence the efficiency of the WPT system. Hence, this paper gives step by step procedure for coil selection and the parameters that influences its performance.

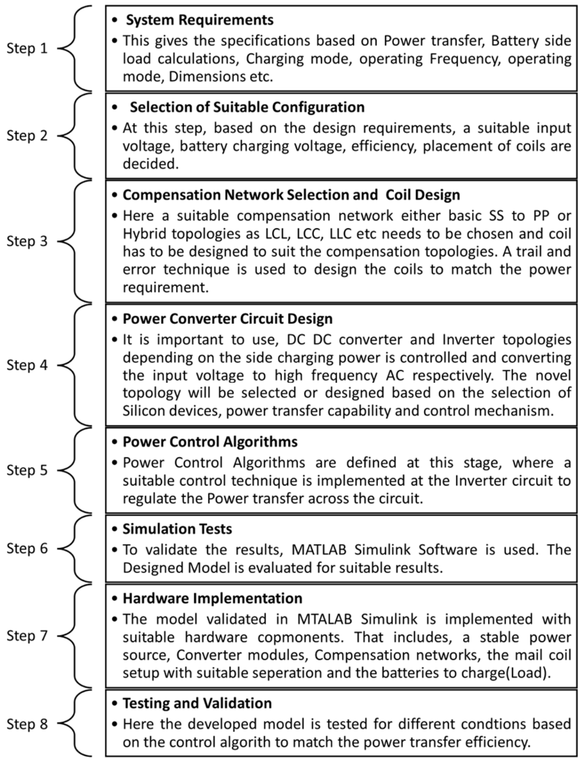

Figure 2. Design Procedure of 3.7 kW WPT charger

A. Requirement Specifications

As the first step in the design procedure, the main components of the WPT systems are defined. Here, Energy flow will always happen from source(grid) to the load as shown in fig 3. but while calculating the power to be transferred, calculations should happen from load to source.

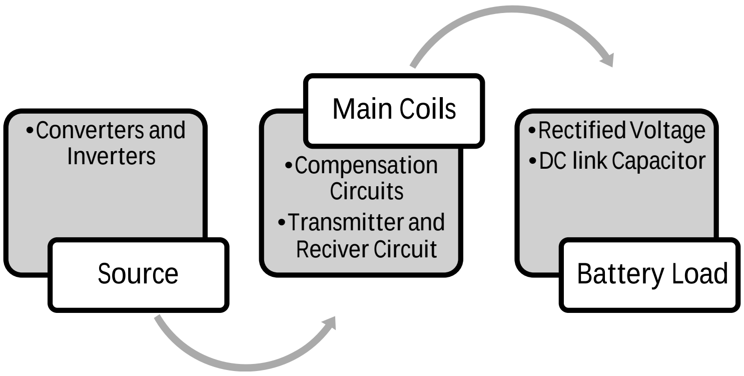

Figure 3. Energy Flow to the Battery

Electrical Specifications:

The coils of Wireless charger system at 3.7 kW is designed according WPT 1 standard. For a nominal charging voltage i.e., output voltage Vo of 84 V, the electrical parameters are calculated. The RMS value of the fundamental component of the primary voltage VP is assumed to be 240 V, since a 3.7 kW charger falls into the category of an AC level 2 charger according to SAE J1772 charging standards and A resonant frequency f_0 of 85 kHz is selected. According to SAE standards. A current of 42A is designed at the output side of the circuit. Total Battery Pack Voltage of 73.6 V with total capacity 288 Ah is selected which is giving a Battery Pack Energy of 21.2 kWh. The Selected Battery Cell Type is Prismatic with 23S4P Configuration. Each Cell is Rated at 3.2 V(Nominal), 72 Ah.

As the chosen resonant frequency is 85 kHz, due to eddy currents, increase in resistance of the wire is noticed. Skin effect and Proximity effect [28 - 31] causes Eddy Current. Braided enameled conductors recognized as Litz wire have been found very effective in mitigating skin effect and proximity effect which is considered as high frequency effects [32 - 34]. A Litz wire consists of several thin strands, each individually insulated, coiled into a wire. The strands are then woven together so that the location of each strand alternates between the center of the wire and the edge of the wire. This ensures that the proximity effect will for each strand will remain the same, and thus carry the same amount of current. The following sections discusses the selection of the number of strands, the wire gauge, and the construction of the Litz wire used in making the coils for the 3.7 kW charger.

Design of Litz-Wire for the Coils:
For the design of Litz-wire the maximum current of 42 A (RMS) is considered to allow the safety margin and future development of the work in this area. To calculate overall gauge of the wire and the required number of strands the following steps are followed:

To find the Complete Gauge of the Wire: Design of Litz wire begins by selecting a correct value of current density for the wire. From the literature [35 - 38], it is *found* that the recommended value of the average current density for a given continuous power level and increase in temperature over ambient temperature for convention cooling lies between 2 to 6 A/mm2. In this paper, a value of 4 A/mm2 is considered. Therefore, for a selected value of the current, the area of the cross section of the wire is given by (2.1).

$$Area\ of\ cross\ section\ of\ wire = \frac{Current}{Current\ Density} \qquad (2.1)$$

Equation (2.1) gives a value of 10.5 mm^2. To allow some safety margin, SWG of 8 with area of cross section 12.97 mm^2, with a wire diameter of 4 mm is selected.
Litz wire has a number of Strands: How to find them [39]: The depth of the skin for a fine conductor is as below,

$$\delta = \sqrt{\frac{\rho}{\pi f \mu}} \qquad (2.2)$$

Where, δ = skin depth in m, f =frequency in Hz, μ = magnetic permeability of the conductor in H/m, ρ = resistivity of the conductor in Ω-m. Frequency = 85000 Hz, permeability = 4π×10-7 Hm, and the value of resistivity of copper = 1.72×10-8 Ω-m [40]. Substituting all the values, Skin depth = 0.2264 mm.
The diameter of a strand must be less than the skin depth. A good design uses a strand diameter smaller than the skin depth by a factor of 4 as discussed in [41]. Therefore, a strand of 41 SWG (0.1118mm) diameter is selected. The number of strands is given by (2.3).

$$\text{Number of Strands} = \frac{\text{Area of Cross Section of Wire}}{\text{Area of Cross Section of individual strand}} \qquad (2.3)$$

Equation (2.3) gives a value of 1323 .46 ~ 1324 number of Strands.
Grouping and bundling of Litz Wire: In the chosen Litz wire, high frequency effects are further classified into strand-level and bundle-level effects [42]. Simple twisting method is acceptable to eliminate the bundle-level proximity effect but to evade bundle level skin effect, multiple levels of twisting, also known as true Litz Wire construction are required [41 – 43]. Initially n1 number of strands are twisted together, followed by twisting n2 sub-bundles and additional stages are followed if required.
The n1 value is as below (2.4) [39].

$$n1 = \frac{4\ x\ (Skin\ Depth)^2}{(Diameter\ of\ Single\ Strand)^2} \qquad (2.4)$$

From (2.4), n1 is calculated as 16.40 ~ 16. 16 Strands are twisted and bundled at the first level to eliminate the bundle skin effect. Three, Four and five sub bundles are selected for second level. In this paper, a value of five is used and the second level of twisting gives 5×16 = 80 strands. And, for the next level, 5 bundles of the second level have given 400 strands. Finally, last level 5 bundles of 400 Strands are considered. In the cabling operation, twisting direction at each level alternates and the final construction is designated as 5x5x5x16. The cabling operation is more effective in eliminating high-frequency effects as the selected frequency is 85kHz. Therefore, 8 SWG 5×5×5×16 with single Nylon Served is selected as a Litz Wire.

Coil Design

Magnetic resonance based WPT system works on the principle of transformer where magnetic field is required to transfer power from the source to the load. The magnetic coupler, namely the Transmitter and Receiver coils, plays a important role in the power transmission. The design principles for the magnetic coupler must include: 1) most of the magnetic flux generated by the Transmitter coil should be linked to the Receiver coil, 2) the leakage magnetic flux should be well guided and not affect adjacent environment and 3) Overall a high transfer efficiency is expected to be maintained with reduced material weight and the cost. Coils are generally divided into air core coils and coils with magnetic cores (Ferrites). Air core coils are applied where shielding and electromagnetic interference (EMI) issues have no consideration. In high-power applications, the magnetic field should normally be guided, and EMI issues should be considered. Therefore, coils with magnetic cores are normally adopted [44].

With magnetic cores, accurate analytical expressions for self and mutual inductances can hardly be obtained. Finite element simulation – Ansys Electromagnetics is normally used to acquire the equivalent circuit parameters and the field distribution.

According to different coil types, coils used in high-power Wireless Power Transfer systems are categorized as shown in Fig. 4[45].

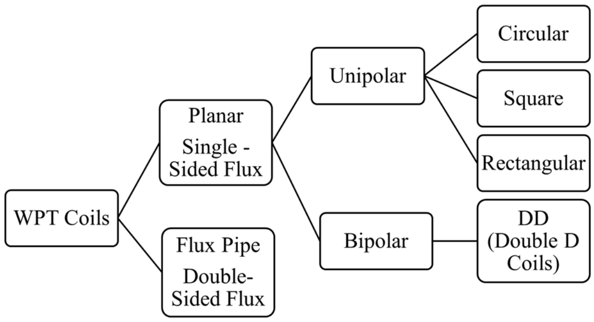

Figure 4. WPT Coil Categories

In WPT Charging systems, Flat planar coils are used to maintain a low-profile structure. In stationary WPT charging systems, two kinds of coils are used, flux pipe coils with double-sided flux and planar coils with single-sided flux. The first type coils are flat solenoid structures. The copper or Litz wire are wounded around the ferrite structure. The coupling coefficient of flux pipe structure is larger than the planar coils [46 – 47]. Sometimes, the magnetic flux is four times larger than planar coils [46] in Flux Pipe structure and requires thick cores to prevent saturation. The magnetic flux cannot be guided only on one side of the ferrite bar. The leakage magnetic flux on the other side of the WPT charging system may affect nearby metal objects, such as chassis and other metal substances that in turn induces Eddy currents in them, causing extra loss, which is significant in high-power WPT charging systems. Also, the parameters of the WPT charging system would be easily affected, and detuning of the resonance can occur. Additional shielding material must be added on the other side to shield the WPT charging system, but this increases the cost and weight, which is crucial for high-power WPT charging systems. Hence, flux pipes are seldom used in high-power WPT charging systems.

Planar coils are flat coils with copper or Litz windings on the same side of the ferrite plate. The magnetic flux is guided by the ferrite plate and the leakage magnetic flux on the other side of the ferrite plate is very low. Aluminium plates are added on the other side of the ferrite plate for better shielding. Therefore, planar coils are highly used type of coils in high-power WPT charging systems. These Planar coils in turn are divided into unipolar coils and bipolar coils. Unipolar coils are further classified into circular coils, square coils, and rectangular coils based on the shape of the pole. Normally in bipolar coils, the shape of the pole is square or rectangular where later is also called DD coils [45]. In this paper Planar Circular and Square coils are compared with Rectangular Bipolar coil. The analysis is carried out with only bare coils, then with ferrites and with ferrites and Aluminium shielding. The transmitter and Receiver coils are placed at 180mm and a parametric Analysis is carried out where distance is varied from 80mm to 180 mm in steps of 50mm using ANSYS Maxwell FEM software.

Planar Coil Simulations

In a typical scenario, WPT inductors may include circular, square and Double D (DD) coil configurations/shapes. However, it is yet to be established that the value of the coupling coefficient can be improved by any of these coil configurations. Therefore, it is necessary to analyze the performance of selected coils in terms of the coupling coefficient. To compare the performance of different coil configurations, ANSYS Maxwell 3D Software was utilized. Structures of circular, square and DD coil configurations with three different scenarios have been compared, Bare coils, Coils with Ferrites and Coils with Ferrites and Aluminium Shielding. The Bare coil structures with transmitter coil and Receiver coil have been presented in Fig 5. In this paper the air-gap distance is fixed at 180 mm as the minimum chassis distance in any Passenger 4-Wheeler ranges between 170 – 190 mm.

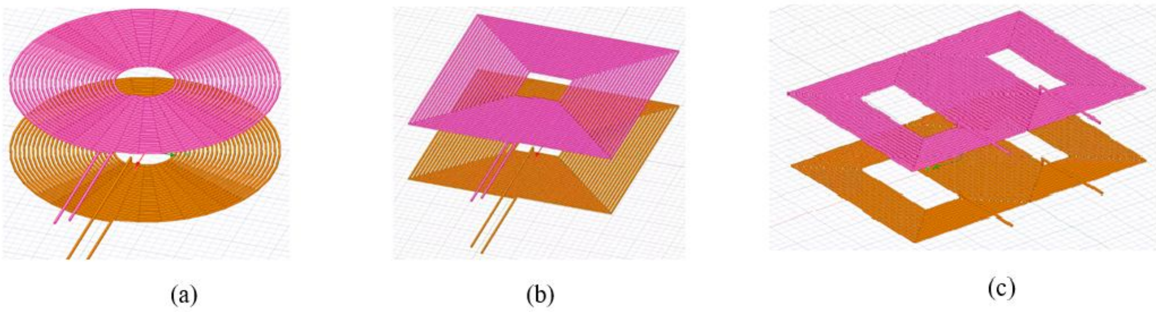

Figure 5. Diagrams of the different Bare coil models: (a) Circular; (b) Square; (c) Double D (DD)

The Dimensions of various coils considered for analysis are as shown are as shown in Table I.

TABLE I. DIFFERENT COIL DIMENSIONS

Parameters	**Circular**	**Square**	**Bipolar**
Internal Diameter (di)	129 mm	129 mm	129 mm
External Diameter (de)	597 mm	597 mm	597 mm x 250 mm
Turns Spacing (S)	6 mm	6 mm	6 mm
Turn Width(W)	4 mm	4 mm	4 mm
No of Transmitter Turns(N1)	24	24	24
No of Receiver Turns(N2)	24	24	24
Airgap Distance	180 mm	180 mm	180 mm

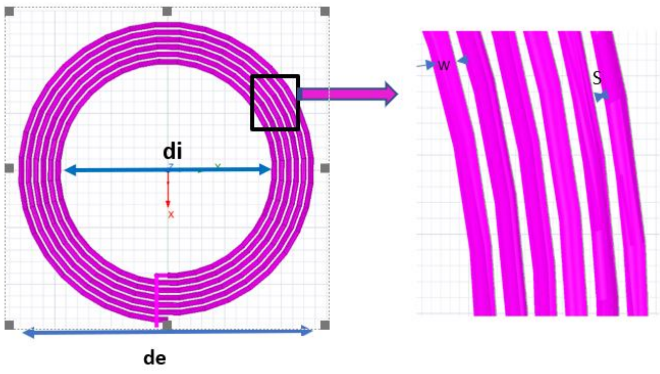

Figure 6. Circular Coil and its Dimensions

Figure 6. shows the dimensions of a circular coil in terms of, di, de, W and S. Where, di is the internal diameter of a coil, de is the external diameter, W is the width of the turn and S is the spacing between the turn.
In WPT charging system, coil optimization plays a vital role to improve the system efficiency. So, it's important to study, compare and analyze the impact on coupling co efficient and efficiency on different coil geometries by changing various its parameters in an iterative process.
The coupling coefficient, self-inductance and Mutual inductance are the key factors to achieve high coupling between two coils. These coils are impacted by its position, addition of flux directional components and coil structural parameters. The analysis of the factors by analytical method is highly complex, time consuming and

may not be accurate sometimes. Finite element analysis is one of the best methods to analyze these coils with near accurate results. Finite analysis method is one of the numerical methods based on determining appropriate solutions. In this method, the whole structure is subdivided into small pieces to generate simple equation system. The solutions of these simple equations are combined to achieve the final solution. Ansys Maxwell is one of the Powerful tools with finite element analysis allowing to evaluate electromagnetic component design. In this paper, a comparative approach is proposed to simulate different coil structures using Ansys FEM Technique.
Table II. gives the Simulation results of Circular, Square and Bipolar DD Coils. The results show the variation of coupling coefficient, Self and Mutual inductances with respect to varying distances.

TABLE II. SIMULATION RESULTS OF BARE COILS

Circular Coils					
dist [mm]	**k**	**L1(μH)**	**M(μH)**	**L2(μH)**	**Flux(Wb)**
80	0.463703217	166.4896275	77.1863945	166.4233	0.0024368
130	0.330929406	180.8768959	59.8149663	180.62	0.0024069
180	0.237228981	184.7321577	43.8079411	184.5983	0.0022854
230	0.171519849	186.4177052	31.963184	186.2877	0.0021838
Square Coils					
80	0.456435568	190.3739122	86.8858423	190.3407	0.0027726
130	0.334068165	208.1521512	69.5434479	208.1907	0.002777
180	0.245382449	213.5455397	52.394168	213.4953	0.0026594
230	0.192528181	215.439258	41.4801965	215.4607	0.0025692
Bipolar Rectangular Coils					
80	0.347097243	94.59076186	33.0109383	95.62351	0.001276
130	0.196343566	94.61703173	18.7013935	95.88381	0.0011332
180	0.115411072	94.48165217	10.982607	95.84478	0.0010546
230	0.069771872	94.48347905	6.64088873	95.88171	0.0010112

The simulation results using ANSYS has demonstrated variation of Coupling Coefficient(k), Self-Inductance (L), Mutual Inductance (M) and Flux with respect to varying distances as shown in figures 7, 8, 9 and 10 respectively.

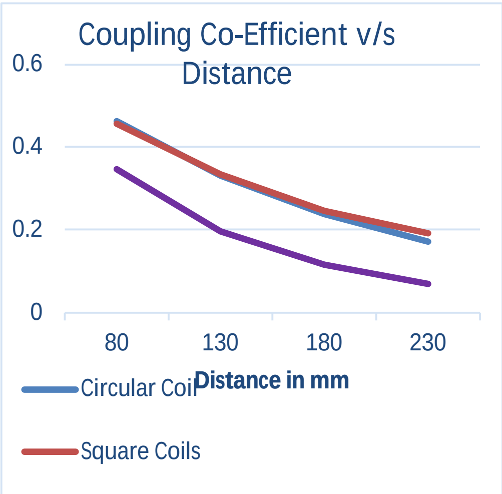

Figure 7. Coupling Coefficient v/s Distance

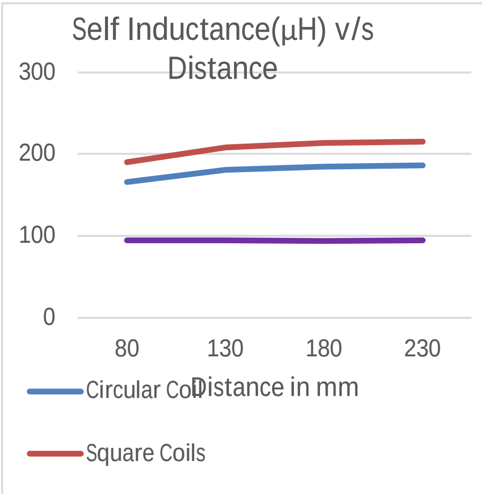

Figure 8. Self-Inductance v/s Distance

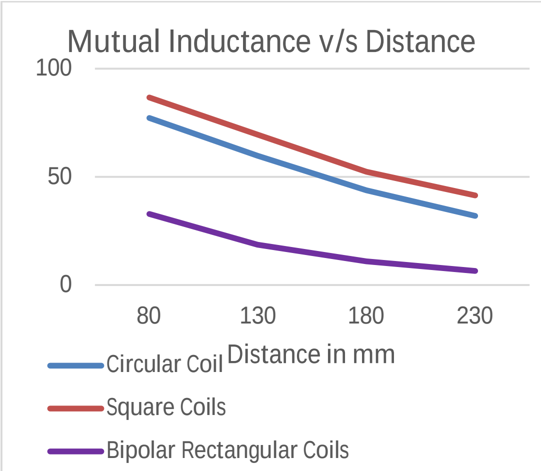

Figure 9. Mutual Inductance v/s Distance

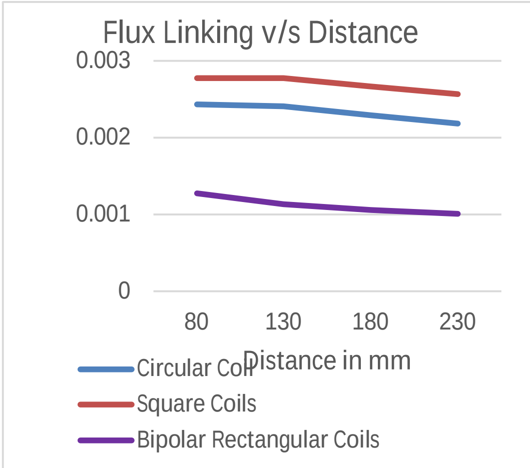

Figure 10. Flux in Wb v/s Distance in mm

From Bare coil analysis it is clear that, the behaviour of Unipolar Circular and Square coils are similar and DD coil behaviour is different.

Figure 11. explains the Magnetic Flux behaviour between Transmitter and Receiver of selected coil structures at 180mm Distance.

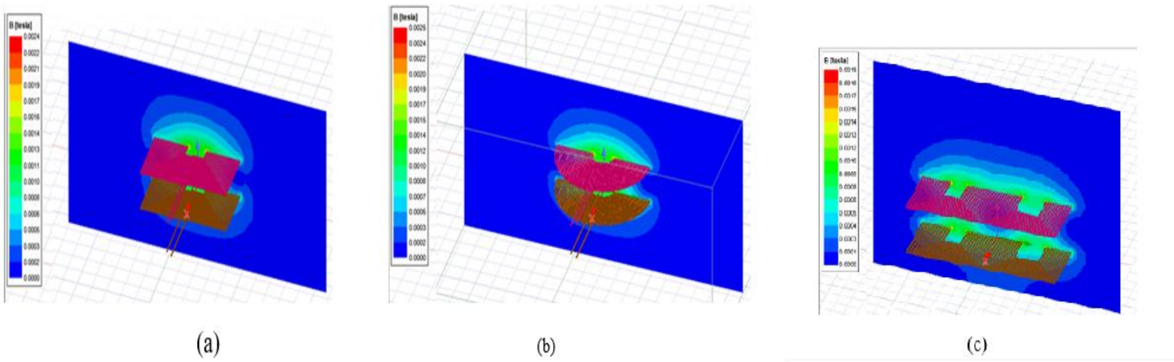

Figure 11. Magnetic Flux linking between Transmitter and Receiver Coils. (a) Circular Coil; (b) Square Coil; (C) Bipolar DD Coil

Similarly, table III. Gives clear comparison of selected coils with Ferrites. The ferrite plate of 2 mm is considered, and length and breadth of the plates matches with respective coil Dimensions.

TABLE III. SIMULATION RESULTS OF COILS WITH FERRITES

Circular Coils					
dist [mm]	**k**	**L1**	**M**	**L2**	**Flux(Wb)**
80	0.713208	421.5563598	300.63557	421.4954	0.0072219
130	0.510374	360.4817842	183.95356	360.3759	0.0054444
180	0.357559	339.1203072	121.2425	339.0475	0.0046036
230	0.250619	330.0617037	82.714407	330.0185	0.0041278
Square Coils					
80	0.708464	489.1995775	346.58274	489.2064	0.0083578
130	0.51283	418.7075798	214.72273	418.6956	0.0063343
180	0.366344	393.6986292	144.23306	393.7195	0.0053793
230	0.26279	383.0240945	100.6531	383.0115	0.0048368

Bipolar Rectangular Coils					
80	0.589254	220.7451503	129.72432	219.5568	0.0035047
130	0.362248	192.0912457	69.355936	190.8307	0.0026145
180	0.221983	182.9583526	40.475478	181.7152	0.0022343
230	0.019234	163.7832	11.04598	162.7453	0.002001

Table III. shows clearly with the addition of 2mm Ferrite core, how all the parameters have improved with its characteristics. This analysis shows one of the best method to enhance coupling coefficient as permeability of ferrite is high and reduces the reluctance path[48]. These results also show that, coupling coefficient and mutual inductance decreases as distance increases. But these values are increased compared to bare coils.
Figure 12 and 13 shows the enhanced coupling coefficient and Mutual inductance and the behaviour of circular and Square coils are almost similar paving way to choose one of the coil types for future analysis.

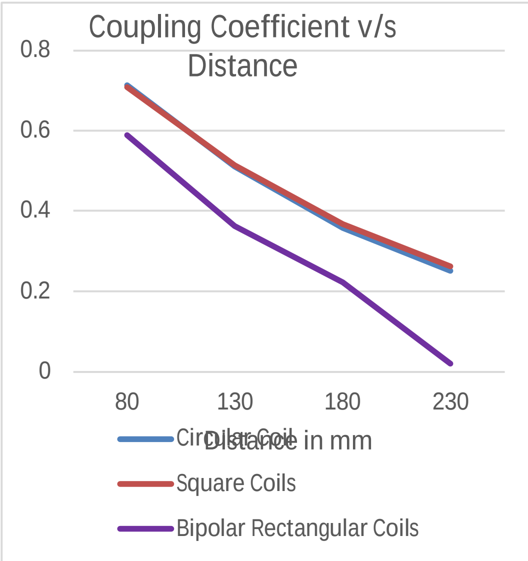

Figure 12. Coupling Coefficient v/s Distance

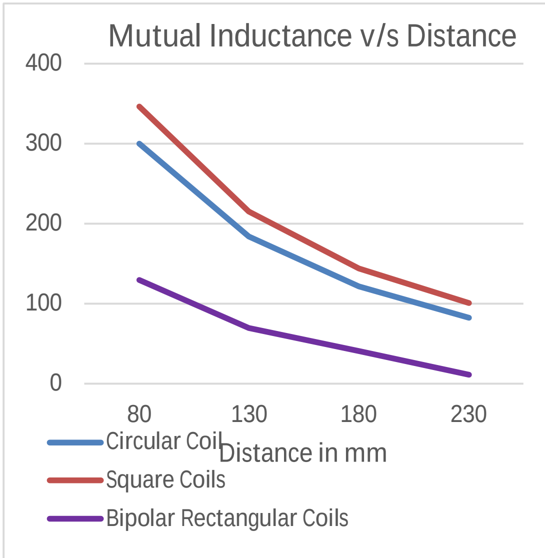

Figure 13. Mutual Inductance v/s Distance

Next level analysis is carried out with Aluminium Plate to analyse its influence on Coupling Coefficient and mutual inductance. Table IV. Summarises the simulation results of coupling coefficient and the mutual inductance with Ferrites and Aluminium plate.

TABLE IV. SIMULATION RESULTS OF COILS WITH FERRITES AND ALUMINIUM

Circular Coils					
dist [mm]	**K**	**L1**	**M**	**L2**	**Flux(Wb)**
80	0.7135185	420.9567	300.3554	420.9427	0.00721312
130	0.5103004	359.5977	183.5056	359.6086	0.00543103
180	0.3573224	338.1904	120.8469	338.2125	0.00459037
230	0.2507536	329.7116	82.67579	329.707	0.00412387
Square Coils					
80	0.7092839	489.6625	347.3077	489.6568	0.0083697
130	0.51343	418.6596	214.9501	418.6506	0.0063361
180	0.3667318	393.408	144.2755	393.4095	0.00537684
230	0.2630762	382.9621	100.7514	382.9865	0.00483714

Bipolar Rectangular Coils					
80	0.5878196	218.551	128.1192	217.3639	0.0034667
130	0.3612147	190.3676	68.54386	189.153	0.00258911
180	0.2216083	181.3548	40.05325	180.1252	0.00221408
230	0.1393883	177.8985	24.70989	176.6511	0.00202608

It can be concluded by looking into different cases of bare oils, coils with ferrites and coils with ferrites and Aluminium, the coil with ferrites is one of the best solution to enhance coupling coefficient and Mutual Inductance. The introduction of Aluminium Shielding plate to three coil structures reduces very marginally coupling coefficient, other values remain relatively high. While maintaining the shielding effect in the ferrite, it is possible to reduce the variation in parameters. Also, the Aluminium plate and thickness of the Aluminium shielding must be greater than the Skin depth [49-50]. Aluminium Shielding also protects users from continuous exposure of magnetic field according to guidance of the ICNIRP standard [51]. Hence Coil structures with ferrites and Aluminium exhibit a merged characteristic with enhanced coupling coefficient and better shielding effects.

III. Conclusions

This Paper discusses the coil design and selection of suitable coil structure for 3.7 kW wireless power transfer charging system and the factors that affect coil performance in terms of Coupling coefficient and Mutual Inductance. The following points were discussed: first, the bare coils are studied, and their performance is observed at varied distances, the influence of adding a ferrite core and aluminium sheet to the coil system is discussed. The result shows that the ferrite and aluminium are necessary to guide the magnetic flux, reduce the leakage flux, protect the users from Magnetic field influence and meet ICNIRP limits. Second, the large air gap reduces the coupling coefficient and mutual inductance values. The main challenge while designing the wireless power transfer charger for the electric vehicle is the distance limitation between the Tx and Rx. This distance depends on the electric vehicle ground clearance and the specifications given by SAE J2954 standard. Third, the coil parameters such as inner radius and number of turns have a significant effect on the system coupling, self-inductance, and mutual inductance. Finally, the comparison of three coil shapes, including ferrite and aluminium, gives priority to the Square shaped Coil, with a small difference compared to the circular and considerable difference with Bipolar Rectangular shapes. Thus, several coil structure possibilities can be encountered during the wireless charging operation. In this paper, with the use of the three coil structures, circular, Square, and Bipolar Rectangular, it can be concluded that the square coil gives the best results with Coupling coefficient and Mutual Inductance.

Further, research concentrates on the choosing the Novel coil structure, loss analysis and hardware implementation and testing. During the loss analysis variation in the parameters will be considered to maintain the optimum efficiency. Moreover, the human safety issue will be taken into consideration during the design process, especially when the power transfer level is increased.

References

[1] Ahson SA, Ilyas M. RFID handbook: applications, technology, security, and privacy. Boca Raton, FL: CRC; 2008.

[2] Covic GA, Boys JT, Kissin MLG, Lu HG. A three-phase inductive power transfer system for roadway-powered vehicles. IEEE Trans Ind Electron Dec. 2007;54(6):3370–8.

[3] Keeling NA, Boys JT, Covic GA. Unity power factor inductive power transfer pick-up for high power applications//2008. In: 34th annual conference of IEEE Industrial Electronics. IEEE; 2008. p. 1039–44.

[4] Budhia M, Covic G, Boys J. A new IPT magnetic coupler for Electric vehicle charging systems. In: Proc. 36t IEEE IECON; 2010. p. 2487–92.

[5] Budhia M, Covic GA, Boys JT. Design, and optimisation of magnetic structures for lumped inductive power transfer systems. In: Proc. IEEE ECCE; 2009. p. 2081–8.

[6] Zhen NL, Chinga RA, Tseng R. Design and test of a high-power high efficiency loosely coupled planar wireless power transfer system. IEEE Trans Ind Electron 2009;56(5):1801–12.

[7] Zhen NL, Casanova JJ, Maier PH. Method of load/fault detection for loosely coupled planar wireless power transfer system with power delivery tracking. Ind Electron IEEE Trans 2010;57(4):1478–86.

[8] Moradewicz AJ, Kazmierkowski MP, Contactless energy transfer system with FPGA-Controlled resonant converter. Ind Electron IEEE Trans 2010;57(9):3181–90.

[9] Jiang WX, Chin JY, Li Z. Analytical design of conformally invisible cloaks for arbitrarily shaped objects. Phys Rev E Stat Nonlinear Soft Matter Phys 2008;77(6 Pt 2):066607.
[10] [Mi, C.C.; Buja, G.; Choi, S.Y.; Rim, C.T. Modern Advances in Wireless Power Transfer Systems for Roadway Powered Electric Vehicles. IEEE Trans. Ind. Electron. 2016, 63, 6533–6545.
[11] Ghosh, A. Possibilities and Challenges for the Inclusion of the Electric Vehicle (EV) to Reduce the Carbon Footprint in the Transport Sector: A Review. Energies 2020, 13, 2602.
[12] González Palencia, J.C.; Nguyen, V.T.; Araki, M.; Shiga, S. The Role of Powertrain Electrification in Achieving Deep Decarbonization in Road Freight Transport. Energies 2020, 13, 2459.
[13] Xiaoli, S.; Zhengguo, L.; Xiaolin, W.; Chengjiang, L. Technology Development of Electric Vehicles: A Review, Energies 2020, 13, 90.
[14] De Santis, M.; Agnelli, S.; Patanè, F.; Giannini, O.; Bella, G. Experimental Study for the Assessment of the Measurement Uncertainty Associated with Electric Powertrain E_ciency Using the Back-to-Back Direct Method. Energies 2018, 11, 3536.
[15] Miller, J.M.; Jones, P.T.; Li, J.M.; Onar, O.C. ORNL experience and challenges facing dynamic wireless power charging of EV's. IEEE Circuits Syst. Mag. 2015, 15, 40–53.
[16] Li, S.; Liu, Z.; Zhao, H.; Zhu, L.; Shuai, C.; Chen, Z. Wireless Power Transfer by Electric Field Resonance and Its Application in Dynamic Charging. IEEE Trans. Ind. Electron. 2016, 63, 6602–6612.
[17] Kim, M.; Kim, K.A.; Kim, J.; Jung, J.H. Design Methodology of a 500WWireless Power Transfer Converter in Proceedings of the 2015 IEEE PELS Workshop on Emerging Technologies Wireless Power (WoW), KAIST, Daejeon, Korea, 5–6 June 2015; p. 6.
[18] Li, W.; Zhao, H.; Deng, J.; Li, S.; Mi, C.C. Comparison Study on SS and double-sided LCC compensation topologies for EV/PHEVWireless Chargers. IEEE Trans. Veh. Technol. 2016, 65, 4429–4439.
[19] Sohn, Y.H.; Choi, B.H.; Lee, E.S.; Lim, G.C.; Cho, G.H.; Rim, C.T. General Unified Analyses of Two-Capacitor Inductive Power Transfer Systems: Equivalence of Current-Source SS and SP Compensations. IEEE Trans. Power Electron. 2015, 30, 6030–6045.
[20] Aditya, K.; Williamson, S.S. Comparative Study of Series-Series and Series-Parallel Compensation Topologies for Electric Vehicle Charging. In Proceedings of the 2014 IEEE 23rd International Symposium on Industrial Electronics (ISIE), Istanbul, Turkey, 1–4 June 2014; IEEE: Piscataway, NJ, USA, 2014; pp. 426–430.
[21] Zhang, W.; Wong, S.C.; Tse, C.K.; Chen, Q. Analysis and comparison of secondary series-and parallel-compensated inductive power transfer systems operating for optimal efficiency and load-independent voltage-transfer ratio. IEEE Trans. Power Electron. 2014, 29, 2979–2990.
[22] Stielau, O.H.; Covic, G.A. Design of loosely coupled inductive power transfer systems. In Proceedings of the 2000 International Conference on Power System Technology, Perth, WA, Australia, 4–7 December 2000; IEEE: Piscataway, NJ, USA, 2000; pp. 85–90.
[23] Neath, M.J.; Swain, A.K.; Madawala, U.K.; Thrimawithana, D.J. An optimal PIDcontroller for a bidirectional inductive power transfer system using multiobjective genetic algorithm. IEEE Trans. Power Electron. 2014, 29, 1523–1531.
[24] Wu, H.H.; Covic, G.A.; Boys, J.T.; Robertson, D.J. A series-tuned inductive-power-transfer pickup with a controllable AC-voltage output. IEEE Trans. Power Electron. 2011, 26, 98–109.
[25] Ravikiran V.; Keshri, R.K.; Santos, M.M.: Inductive characteristics of asymmetrical coils for wireless power transfer. In: Eighteenth annual IEEE international conference on industrial technology, ICIT, Toronto, ON, pp. 538–542 (2017).
[26] Tejeda, A.; Carretero, C.; Boys, J.T.; Covic, G.A.: Ferrite-less circular pad with controlled flux cancelation for EVwireless charging. IEEE Trans. Power Electron. 32(11), 8349–8359 (2017).
[27] Zaheer, A.; Hao, H.; Covic, G.A.; Kacprzak, D.: Investigation of multiple decoupled coil primary pad topologies in lumped IPT systems for interoperable electric vehicle charging. IEEE Trans. Power Electron. 30(4), 1937–1955 (2015).
[28] Kim, S.; Covic, G.A.; Boys, J.T.: Tripolar pad for inductive power transfer systems for EV charging. IEEE Trans. Power Electron. 32(7), 5045–5057 (2017).
[29] A. E. Ruehli, G. Antonini and L. Jiang, "Skin-effect model for round wires in PEEC," in Proc. IEEE International Symposium on Electromagnetic Compatibility, Rome, 2012, pp. 1-6.
[30] P. Meyer and Y. Perriard, "Skin and proximity effects for coreless transformers," in Proc. IEEE International Conference on Electrical Machines and Systems, Beijing, 2011, pp. 1-5.
[31] M. Bartoli, A. Reatti and M. K. Kazimierczuk, "High-frequency models of ferrite core inductors," in Proc. IEEE International Conference on Industrial Electronics, Control and Instrumentation, Bologna, 1994, pp. 1670-1675 vol.3.
[32] S. Mei and Y. I. Ismail, "Modeling skin and proximity effects with reduced realizable RL circuits," in IEEE Transactions on Very Large-Scale Integration (VLSI) Systems, 2004, vol. 12, no. 4, pp. 437–447.
[33] J. Mühlethaler, J. W. Kolar and A. Ecklebe, "Loss modeling of inductive components employed in power electronic systems," in Proc. IEEE 8th International Conference on Power Electronics and ECCE Asia, Jeju, 2011, pp. 945-952.
[34] R. Bosshard, J. W. Kolar, J. Mühlethaler, I. Stevanović, B. Wunsch, and F. Canales, "Modeling and η - α-pareto optimization of inductive power transfer coils for electric vehicles," IEEE Journal of Emerging and Selected Topics in Power Electronics, vol. 3, no. 1, pp. 50-64, March 2015.
[35] C. R. Sullivan, "Optimal choice for number of strands in a litz-wire transformer winding," IEEE Trans. on Power Electronics, vol. 14, no. 2, pp. 283–291, 1999.

[36] J. Sallan, J. L. Villa, a. Llombart, and J. F. Sanz, “Optimal Design of ICPT Systems Applied to Electric Vehicle Battery Charge,” IEEE Trans.on Industrial Electronics, vol. 56, no. 6, pp. 2140–2149, 2009.
[37] J. M. Miller and A. Daga, “Elements of Wireless Power Transfer Essential to High Power Charging of Heavy-Duty Vehicles,” IEEE Trans. on Transportation Electrifications, vol. 1, no. 1, pp. 26–39.
[38] M. Hediehloo and M. Akhbari, "New approach in design of planar coil of induction cooker based on skin and proximity effects analysis," in Proc. IEEE International Conference on Industrial Technology, Gippsland, VIC, 2009, pp. 1-6.
[39] A. E. Ruehli, G. Antonini and L. Jiang, "Skin-effect model for round wires in PEEC," in Proc. IEEE International Symposium on Electromagnetic Compatibility, Rome, 2012, pp. 1-6.
[40] M. Hediehloo and M. Akhbari, "New approach in design of planar coil of induction cooker based on skin and proximity effects analysis," in Proc. IEEE International Conference on Industrial Technology, Gippsland, VIC, 2009, pp. 1-6.
[41] C. R. Sullivan and R. Y. Zhang, "Simplified design method for litz wire," in Proc. IEEE Applied Power Electronics Conference and Exposition, Fort Worth, TX, 2014, pp. 2667-2674.
[42] C. R. Sullivan, “Optimal choice for number of strands in a litz-wire transformer winding,” IEEE Trans. on Power Electronics, vol. 14, no. 2, pp. 283–291, 1999.
[43] C. R. Sullivan, “Cost-constrained selection of strand diameter and number in a litz-wire transformer winding,” IEEE Trans. on Power Electronics, vol. 16, no. 2, pp. 281–288, 2001.
[44] D. Wu, H. Chao, Y. Fan, and S. Qisheng, “Analytical calculations of self-and mutual inductances for rectangular coils with lateral misalignment in IPT,” in IET Power Electronics, vol. 12, no. 15, pp. 4054-4062, Dec. 2019.
[45] Yiming ZHANG, Shuxin CHEN, Xin LI, And Yi TANG, “Design of High-Power Static Wireless Power Transfer Via Magnetic Induction: An Overview”, CPSS Transactions on Power Electronics And Applications, vol. 6, no. 4, december 2021.
[46] R. Haldi, K. Schenk, I. Nam, and E. Santi, “Finite-element-simulation-assisted optimized design of an asymmetrical high-power inductive coupler with a large air gap for EV charging,” in Proceedings of 2013 IEEE Energy Conversion Congress and Exposition, 2013, pp. 3635-3642.
[47] M. Budhia, G. Covic, and J. Boys, “A new IPT magnetic coupler for electric vehicle charging systems,” in Proceedings of IECON 2010 - 36th Annual Conference on IEEE Industrial Electronics Society, 2010, pp. 2487-2492
[48] Elnail, K.; Huang, X.; Xiao, C.; Tan, L.; Haozhe, X. Core Structure and Electromagnetic Field Evaluation in WPT Systems for Charging Electric Vehicles. Energies 2018, 11, 1734.
[49] Geselowtiz, D.B.; Hoang, Q.T.N.; Gaumond, R.P. The Effects of Metals on a Transcutaneous Energy Transmission System. IEEE Trans. Biomed. Eng. 1992, 39, 928–934.
[50] Kim, J.; Kim, J.; Kong, S.; Kim, H.; Suh, I.-S.; Suh, N.P.; Cho, D.-H.; Kim, J.; Ahn, S. Coil Design and Shielding Methods for a Magnetic Resonant Wireless Power Transfer System. Proc. IEEE 2013, 101, 1332–1342.
[51] ICNIRP|LF (1 Hz–100 KHz). Available online: https://www.icnirp.org/en/frequencies/low-frequency/index.html (accessed on 6 September 2020).